HHS Public Access

Author manuscript

Pigment Cell Melanoma Res. Author manuscript; available in PMC 2024 September 01.

Published in final edited form as:

Pigment Cell Melanoma Res. 2023 September ; 36(5): 399–406. doi:10.1111/pcmr.13088.

BMI1 is required for melanocyte stem cell maintenance and hair pigmentation

Molly M. Wilson[1,2], **Paul S. Danielian**[1,#], **Griffin Salus**[1,#], **Roberta Ferretti**[1], **Charles A. Whittaker**[1], **Jacqueline A. Lees**[1,2,*]

[1]David H. Koch Institute for Integrative Cancer Research at MIT, Cambridge, Massachusetts.

[2]Department of Biology, Massachusetts Institute of Technology, Cambridge, Massachusetts.

Abstract

The epigenetic repressor BMI1 plays an integral role in promoting the self-renewal and proliferation of many adult stem cell populations, and also tumor types, primarily through silencing the *Cdkn2a* locus, which encodes the tumor suppressors $p16^{Ink4a}$ and $p19^{Arf}$. However, in cutaneous melanoma, BMI1 drives epithelial-mesenchymal transition programs, and thus metastasis, while having little impact on proliferation or primary tumor growth. This raised questions about the requirement and role for BMI1 in melanocyte stem cell (McSC) biology. Here, we demonstrate that murine melanocyte-specific *Bmi1* deletion causes premature hair greying and gradual loss of melanocyte lineage cells. Depilation enhances this hair greying defect, accelerating depletion of McSCs in early hair cycles, suggesting that BMI1 acts to protect McSCs against stress. RNA-seq of McSCs, harvested before onset of detectable phenotypic defects, revealed that *Bmi1* deletion derepresses $p16^{Ink4a}$ and $p19^{Arf}$, as observed in many other stem cell contexts. Additionally, BMI1 loss downregulated the glutathione S-transferase enzymes, *Gsta1* and *Gsta2*, which can suppress oxidative stress. Accordingly, treatment with the antioxidant N-acetyl cysteine (NAC) partially rescued melanocyte expansion. Together, our data establish a critical function for BMI1 in McSC maintenance that reflects a partial role for suppression of oxidative stress, and likely transcriptional repression of *Cdkn2a*.

Keywords

Melanocytes; Stem Cells; Epigenetic Repression; Hair Follicle; Polycomb Repressive Complex 1

Mouse coat color is coordinated by melanocytes in the hair follicle that synthesize melanin pigment (Nishimura, 2011). During murine embryonic development, a subset of neural crest cells specify as melanoblasts, which are precursors to both self-renewing, undifferentiated melanocyte stem cells (McSCs) and terminally differentiated melanocytes (Mort et al., 2015). Subsequently, melanoblasts migrate to the developing hair follicle, where they populate two distinct locations and undergo further fate specification. Melanoblasts that reach the hair follicle stem cell niche, the bulge, give rise to quiescent McSCs, while those

*Corresponding Author: jalees@mit.edu.
#These authors contributed equally to this work.

Competing Interests: The authors declare no conflict of interest.

populating the lower region of the developing follicle, the bulb, differentiate into mature melanocytes. Throughout life, the hair follicle cyclically progresses through a growth phase (anagen), regression phase (catagen), and resting phase (telogen) (Alonso & Fuchs, 2006). Melanocyte biology is tightly linked to these hair cycles (Steingrímsson et al., 2005). During anagen, McSCs, or melanoblasts for the first hair cycle, give rise to melanocytes that transfer melanin to keratinocytes in the bulb, which compose the new hair shaft. As the hair shaft stops growing, the follicle enters catagen, and apoptosis of melanocytes and keratinocytes in the bulb causes recession of the follicle, leaving only the lower permanent portion of the follicle, including the bulge and resident McSCs. McSCs remain quiescent in the bulge during telogen until activating signals from the microenvironment trigger the transition into anagen again (Rabbani et al., 2011).

Defects in melanoblast survival and expansion during hair follicle morphogenesis and/or McSC maintenance during hair cycles can lead to a reduction in melanocytes and hair pigmentation. Numerous mouse models have highlighted key genes and processes required for maintenance of melanocyte lineage cells. Melanocyte lineage-specific deletion of *c-Myc* during embryogenesis disrupts proliferation of melanoblasts, and reduces the number of McSCs and melanocytes colonizing the developing hair follicle (Pshenichnaya et al., 2012). In contrast, melanoblast-specific deletion of the anti-apoptotic factor *Bcl2* allows melanocyte establishment within the hair follicle, but causes McSCs to apoptose as they enter dormancy (Nishimura et al., 2005). Additionally, genotoxic stress, caused by deletion of *ATM* or irradiation, causes McSCs to differentiate in the bulge and yield ectopically pigmented melanocytes (Inomata et al., 2009). In each case, the premature loss of melanocyte lineage cells manifests as hair greying.

The proto-oncogene BMI1 is a critical regulator of stem cell function. Much of our understanding of BMI1's role in tissue development and homeostasis has been elucidated by studies of germline $Bmi1^{-/-}$ mice (van der Lugt et al., 1994). These mice have shortened lifespans, and demonstrate neurological and hematopoietic defects that are primarily due to inadequate tissue stem cell maintenance (Iwama et al., 2004; Lessard & Sauvageau, 2003; Park et al., 2003). Canonically, BMI1 promotes self-renewal and proliferation through transcriptional silencing of the *Cdkn2a* locus, which encodes the tumor suppressors $p16^{Ink4a}$ and $p19^{Arf}$ (Jacobs et al., 1999a). Derepression of *Cdkn2a* transcription causes cell cycle arrest, senescence, or apoptosis. Accordingly, the stem cell defects in $Bmi1^{-/-}$ neural, hematopoietic, bronchioalveolar, and mammary tissues are ameliorated by deletion of $p16^{Ink4a}$ and/or $p19^{Arf}$ (Dovey et al., 2008; Molofsky et al., 2005; Oguro et al., 2006; Pietersen et al., 2008). BMI1 has other non-canonical roles, which are context-dependent, including lineage specification through *Hox* gene silencing, DNA damage response, and reactive oxygen species (ROS) homeostasis (Cao et al., 2005; Ginjala et al., 2011; Liu et al., 2009). Cancer cells often share molecular characteristics with the adult stem cells of the relevant tissue type, including activation of BMI1. Indeed, BMI1 was first identified as an oncogene (van Lohuizen et al., 1991), and it promotes tumorigenesis in a variety of cancer types, largely through *Cdkn2a* silencing, but also other *Cdkn2a*-independent mechanisms (Douglas et al., 2008; Ferretti et al., 2016; Gargiulo et al., 2013; Jacobs et al., 1999b; Mariani et al., 2016). In cutaneous melanoma, we previously found that *Bmi1* deletion has no impact on proliferation or tumor initiation programs, but instead specifically affects

metastasis through a *Cdkn2a*-independent mechanism, involving epithelial-mesenchymal transition (EMT) regulation (Ferretti et al., 2016). This raises the question of whether BMI1 is involved in McSC biology, which has been proposed by others (Fessé et al., 2022; Huang & Hornyak, 2015) and, if true, whether this reflects *Cdkn2a*-dependent or non-canonical roles. Here, we use a mouse model, in which *Bmi1* is deleted in the melanocytic lineage, to evaluate the phenotypic, cellular and molecular consequences of BMI1 loss on melanocyte biology.

In our conditional *Bmi1* mouse model, exons 4 through 8 are flanked by loxP sites (Maynard et al., 2014). We crossed these $Bmi1^{fl}$ mice with ones carrying a *Tyr*-Cre allele (Tonks et al., 2003) to generate homozygous $Bmi1^{fl/fl}$ mice with *Tyr*-Cre to induce *Bmi1* deletion (ΔBmi1) during melanocyte lineage specification (Fig. 1A). Mice homozygous $Bmi1^{fl/fl}$ without *Tyr*-Cre typically served as controls (CTL) unless otherwise indicated. CTL and ΔBmi1 mice exhibit similar hair pigmentation at postnatal day 10 (P10) and at 7 weeks of age. However, by 6 months of age, ΔBmi1 mice displayed a distinctive hair greying phenotype, which progressed over time (Fig. 1B). As an additional control, we established that $Bmi1^{+/+}$ mice expressing *Tyr*-Cre (n = 5) did not show premature hair greying. Thus, hair greying was specific to BMI1loss and not simply a response to Cre (data not shown).

Mechanical and genotoxic stress, mediated by repetitive depilation or irradiation, promotes hair greying (Inomata et al., 2009; Li & Hou, 2018). Given this, we asked whether the hair greying defect of ΔBmi1 mice is exacerbated by stress. First, we depilated the dorsal hair of CTL and ΔBmi1 mice at P51, allowed hair to grow back until P79 to depilate again, and found that the ΔBmi1 dorsal coat color was notably white at the site of depilation at P206, while CTL mice displayed only minimal greying (Fig. S1A). Second, we depilated CTL and ΔBmi1 mice at P49, to induce a synchronized transition from telogen to anagen, and exposed the mice to irradiation a day later. We allowed the hair to grow back and observed more pronounced hair greying in ΔBmi1, compared to CTLs (Fig. S1B). Collectively, these data support the notion that BMI1 helps to protect McSCs from stress.

We wished to quantify the consequences of BMI1 loss on melanocytic lineage cells over time. Thus, we introduced both a reverse-tetracycline transactivator, driven by the melanocyte lineage *Dct* promoter (*Dct*-rtTA), and H2B-GFP, driven by a tetracycline-responsive element (TRE-H2B-GFP) (Zaidi et al., 2011), into our mouse model. Feeding these animals with doxycycline pellets ad libitum causes melanocyte lineage cells to be marked by nuclear GFP, herein referred to as Dct-GFP (Fig. 1C). To determine whether the hair greying phenotype is linked to melanocyte lineage cell loss, we aged a small cohort of CTL and ΔBmi1 mice to 60 weeks, and found that Dct-GFP^+ cells were significantly less abundant (3.94-fold, $p < 0.0001$) in the hair follicles of ΔBmi1 mice than the CTL counterparts (Fig. 1D, 1E). Thus, melanocyte lineage cells are depleted in ΔBmi1 mice.

Given the known causes of hair greying and BMI1's known role in other stem and progenitor cell populations, we hypothesized that BMI1 was enabling melanoblasts and/or McSCs. Since BMI1 coordinates cell migration programs in cutaneous melanoma, it seemed plausible that BMI1 loss impedes melanoblast colonization and/or expansion, leading to fewer McSCs and melanocytes in the developing hair follicle. To test this hypothesis, we

collected dorsal skin of CTL and ΔBmi1 mice at postnatal day 10 (P10), at which time the hair follicle is in anagen of the first hair cycle, and melanoblasts have given rise to McSCs in the bulge and melanocytes in the bulb (Fig. 2A). Hair follicles are very dense in the mouse skin at P10, making it difficult to identify the specific McSCs and melanocytes that correspond to a single hair follicle. Thus, we quantified the number of Dct-GFP$^+$ cells in the upper and lower halves of a fixed area of hair follicles, designating the upper and lower Dct-GFP$^+$ cells as McSCs and melanocytes, respectively (Fig. 2B). At this P10 timepoint, there was no significant difference in the number of McSCs ($p = 0.5582$) or melanocytes ($p = 0.5847$) in CTL versus ΔBmi1 mice, suggesting that melanoblast migration and expansion are not dependent on BMI1 (Fig. 2C).

Having ruled out a melanoblast defect, we postulated that BMI1 has a role in McSC maintenance in subsequent hair cycles, and that *Bmi1* deletion leads to a gradual loss of McSCs. To address this, we quantified melanocyte lineage cells in the mouse skin during induced anagen and at other timepoints, during the endogenous hair cycle. In anagen of the second hair cycle, which initiates at the end of telogen around P21 (Alonso & Fuchs, 2006), McSCs are activated to divide asymmetrically to self-renew and give rise to differentiating melanocytes. As hair follicles become increasingly asynchronous after the first hair cycle, we began our analysis by depilating the dorsal hair of CTL and ΔBmi1 mice at P21, to induce synchronous entry into anagen of the second hair cycle (Fig. 2D). Skin was then collected at P27 for histological processing and fluorescence microscopy to quantify the Dct-GFP$^+$ McSCs per bulge and melanocytes per bulb (Fig. 2E). We observed significant reductions in both McSCs (1.72-fold, $p < 0.0001$) and melanocytes (2.49-fold, $p < 0.0001$) in ΔBmi1 versus CTL mice (Fig. 2F). To examine whether McSC impairment is amplified by the third hair cycle, we depilated dorsal hair of mice during telogen at P49, collected skin at P55 (corresponding to anagen), and quantified Dct-GFP$^+$ McSCs in the bulge and melanocytes in the bulb (Fig. 2G, 2H). This revealed an even greater reduction in McSCs (2.77-fold, $p < 0.0001$) and melanocytes (3.40-fold, $p < 0.0001$) in the ΔBmi1 animals (Fig. 2I). This progressive decrease in melanocyte lineage cells indicates that BMI1 is required for McSCs to survive to self-renew and differentiate, particularly in response to depilation, suggesting that the *Bmi1* mutant phenotype is exacerbated by stress.

As described above, we observed loss of Dct-GFP$^+$ melanocytic lineage cells at 60 weeks in the absence of depilation. Thus, we wanted to determine whether this was apparent in early hair cycles. First, we quantified the number of Dct-GFP$^+$ melanocyte lineage cells in the skin of CTL and ΔBmi1 mice at P27 without depilation, when the synchrony is incomplete but most hair follicles exist in anagen (Fig. S2A). In this context, there was no significant difference ($p = 0.4487$) in the number of melanocyte lineage cells in ΔBmi1 versus CTL mice, indicating that BMI1 loss alone does not induce melanocyte lineage cell depletion by P27 (Fig. S2B). We also examined mice at P49, when the majority of hair follicles are in telogen of the second hair cycle, such that the melanocytes have undergone apoptosis and the remaining Dct-GFP$^+$ cells are McSCs. Quantification of P49 samples showed a subtle, but not statistically significant ($p = 0.3661$), decrease in the number of ΔBmi1 McSCs (Fig. S2C, S2D). Collectively, our data show that BMI1 is required to support melanocyte lineage cells, and that its absence makes these cells more sensitive to either acute stress resulting from depilation or chronic stress arising during aging. It remains an open question whether,

in response to stress, BMI1 preserves melanocyte lineage cells' proliferative capacity and/or suppresses apoptosis.

As BMI1 is a transcriptional regulator, we wanted to identify transcriptional changes that occurred in the ΔBmi1 McSCs. We chose to conduct this analysis before the onset of significant phenotypic differences between ΔBmi1 and CTL animals, to focus on changes that were more likely to be the cause, rather than consequence, of McSC defects. Thus, we collected skin from CTL and ΔBmi1 mice at P21 in the absence of depilation. Since P21 hair follicles have entered telogen, Dct-GFP$^+$ cells within the hair follicle are McSCs. We dissociated the tissues and used fluorescence-activated cell-sorting (FACS) to isolate CTL and ΔBmi1 Dct-GFP$^+$ cells (Fig. 3A), and then conducted bulk RNA-seq. STAR alignment confirmed that exons 4 through 8 were excised from the *Bmi1* locus exclusively in ΔBmi1 McSCs (Fig. 3B). We identified 52 genes that were significantly differentially expressed between CTL and ΔBmi1 McSCs (Fig. 3C; Supp. Table S1). Among these, the majority were upregulated in the ΔBmi1 samples (39/52), consistent with BMI1's role as an epigenetic repressor. The top upregulated locus in ΔBmi1 McSCs was *Cdkn2a*. We also identified various transcription factors, including *Hoxb13, Tbx15*, *Hlx*, as upregulated, consistent with BMI1's known role in direct silencing of homeobox genes during development. Interestingly, we observed downregulation of *MC1R*, which encodes the melanocyte stimulating hormone receptor, raising the possibility that BMI1 loss impacts normal melanocytic gene programs. Furthermore, *Gsta1* and *Gsta2*, which encode the enzymes glutathione S-transferase alpha (GSTA) 1 and 2 that mediate ROS neutralization were also downregulated. We presume that transcriptional downregulation is an indirect consequence of *Bmi1* deletion, as BMI1 promotes gene silencing. Nonetheless, this result was very intriguing, given BMI1's known, non-canonical role in ROS mediation, and our finding that stress exacerbates the phenotypic consequences of BMI1 loss on McSCs. We sorted new Dct-GFP$^+$ cells from CTL and ΔBmi1 P21 mice, extracted RNA and performed qRT-PCR for *Cdkn2a* and *Gsta1/2*. In agreement with the RNA-seq results, ΔBmi1 McSCs show marked upregulation of $p16^{Ink4a}$ and, to a lesser degree, $p19^{Arf}$ transcripts (Fig. 3D). Moreover, we confirmed *Gsta1/2* downregulation in the two ΔBmi1 samples with the greatest degree of *Bmi1* transcript downregulation.

We decided not to test the effects of introducing $Cdkn2a^{fl/fl}$ alleles into our mouse model, given both the time required for this experiment, and overwhelming evidence for *Cdkn2a*'s role in numerous other *Bmi1*-deficient stem cell populations. Instead, we chose to explore the role of ROS in our *Bmi1*-null mouse model. Specifically, since GSTA1 and GSTA2 neutralize ROS through the conjugation of glutathione, we hypothesized that the observed downregulation of these genes in ΔBmi1 McSCs might promote ROS, and thus cellular stress, which could contribute (potentially in concert with *Cdkn2a* activation) to the observed synergy between BMI1 loss and stress. Given this, we utilized the antioxidant N-acetyl cysteine (NAC), which is a precursor to glutathione, with the rationale that increasing intracellular glutathione might help the lower levels of GSTA1/2 to neutralize ROS, decrease oxidative stress, and potentially modulate McSC survival. Therefore, we administered water supplemented with or without 1 mg/mL NAC to CTL and ΔBmi1 mice from P0-P27. These mice were depilated at P21 to both initiate entry into anagen of the second hair cycle and induce stress, and skin was collected at P27 to enable quantification of McSCs

and melanocytes (Fig. 3E). Consistent with our prior analyses, McSCs per bulge were significantly underrepresented in untreated ΔBmi1 versus CTLs ($p = 0.0011$). CTL mice treated with NAC showed a modest, but significant, decrease in McSCs per bulge compared to untreated CTL mice ($p = 0.0250$). In contrast, NAC did not alter the representation of McSCs per bulge in ΔBmi1 mice ($p = .9963$). Consequently, NAC treatment reduced the difference in the number of McSCs in the ΔBmi1 versus CTL setting ($p = 0.0863$), hinting at some amelioration of the McSC defect. In the case of melanocytes per bulb, these were also significantly depleted in ΔBmi1 versus CTL mice in both untreated and NAC-treated conditions ($p < 0.0001$ for both). However, the NAC-treated ΔBmi1 mice had significantly more melanocytes per bulb than the untreated ΔBmi1 counterparts ($p = 0.0267$). The negative effect of NAC on CTL McSC numbers was unexpected, and further investigation is clearly required. Nevertheless, NAC treatment had the opposite effect on ΔBmi1 melanocytes, yielding a modest recovery in numbers. Overall, our results suggest that NAC improves the survival of ΔBmi1 transit-amplifying cells that differentiate to melanocytes.

Premature differentiation is another common mechanism by which McSCs lose self-renewing capacity and decrease in response to stress (Inomata et al., 2009). In this process, McSCs undergo ectopic differentiation in the bulge, which leads to hair greying (Harris et al., 2013). Thus, we also asked whether ΔBmi1 McSCs undergo premature differentiation in response to depilation, by using Fontana Masson staining to detect melanin in P27 CTL and ΔBmi1 mouse skin treated with or without NAC (Fig. S3). We saw no ectopic pigmented melanocytes in the bulge in any of these conditions. This lack of prematurely differentiated melanocytes, combined with the discovery that depilation causes rapid loss of ΔBmi1 McSCs, suggests that these cells reach an alternate fate. Interestingly, Fessé and colleagues recently reported that BMI1 expression increases in self-renewing interfollicular melanocytes when patients are treated with radiation therapy, and proposed that BMI1 functions to protect these melanocytes by suppressing p53-mediated cell death (Fessé et al., 2022). Therefore, BMI1 loss likely predisposes McSCs to apoptosis, instead of premature differentiation.

Collectively, our experiments show that BMI1 is a critical gene for McSC maintenance and mouse hair pigmentation, at least in part by providing protection from stress. BMI1 is known to be required for stem cell function in many different tissues. While we believe BMI1 is primarily required in McSCs themselves, our data do not exclude the possibility that BMI1 also promotes the proliferative capacity of transit-amplifying cells that expand in the bulb prior to differentiating into melanocytes. We speculate that ΔBmi1 McSCs, and their progeny, have impaired survival largely due to activation of $p16^{Ink4a}$ and $p19^{Arf}$, which promote cell cycle arrest and/or apoptosis, as has been observed in response to embryonic *Bmi1* deletion in many other adult stem cells. In addition, our findings regarding *Gsta1/2* downregulation upon *Bmi1* deletion in McSCs, and the partial rescue of ΔBmi1 melanocytes upon NAC treatment, support a growing body of work revealing a non-canonical role for BMI1 in mitigating oxidative stress (Chen et al., 2015; Liu et al., 2009). Collectively, we have uncovered a critical role for BMI1 in McSC biology that is likely *Cdkn2a*-dependent, as in many other adult stem cell populations, but also seems to reflect regulation of stress responses (Fig. S4).

Supplementary Material

Refer to Web version on PubMed Central for supplementary material.

Acknowledgements

General:

We thank the Robert A. Swanson (1969) Biotechnology Center, and particularly the MIT BioMicro Center (Stuart Levine), Flow Cytometry Core, and Histology Core, for technical support. We also thank I. Tonks and M. Vander Heiden for transgenic mouse alleles.

Funding:

This work was supported by the MIT Stem Cell Initiative through Fondation MIT and the Koch Institute Support (core) grant P30-CA14051 from the National Cancer Institute to the Swanson Biotechnology Center. M.M.W. was supported by the David H. Koch Graduate Fellowship. J.A.L. is a D.K. Ludwig Professor for Cancer Research.

Data and Materials Availability:

All data needed to evaluate the conclusions in the paper are present in the paper and/or the Supplementary Materials. RNA-seq data are available from the Gene Expression Omnibus under accession number GSE194373.

References

Alonso L, & Fuchs E. (2006). The hair cycle. Journal of Cell Science, 119(3), 391–393. 10.1242/jcs.02793 [PubMed: 16443746]

Cao R, Tsukada Y-I, & Zhang Y. (2005). Role of Bmi-1 and Ring1A in H2A ubiquitylation and Hox gene silencing. Molecular Cell, 20(6), 845–854. 10.1016/j.molcel.2005.12.002 [PubMed: 16359901]

Chen Y, Li L, Ni W, Zhang Y, Sun S, Miao D, Chai R, & Li H. (2015). Bmi1 regulates auditory hair cell survival by maintaining redox balance. Cell Death & Disease, 6(1), e1605–e1605. 10.1038/cddis.2014.549

Douglas D, Hsu JH-R, Hung L, Cooper A, Abdueva D, van Doorninck J, Peng G, Shimada H, Triche TJ, & Lawlor ER. (2008). BMI-1 Promotes Ewing Sarcoma Tumorigenicity Independent of *CDKN2A* Repression. Cancer Research, 68(16), 6507–6515. 10.1158/0008-5472.CAN-07-6152 [PubMed: 18701473]

Dovey JS, Zacharek SJ, Kim CF, & Lees JA. (2008). Bmi1 is critical for lung tumorigenesis and bronchioalveolar stem cell expansion. Proceedings of the National Academy of Sciences of the United States of America, 105(33), 11857–11862. 10.1073/pnas.0803574105

Ferretti R, Bhutkar A, McNamara MC, & Lees JA. (2016). BMI1 induces an invasive signature in melanoma that promotes metastasis and chemoresistance. Genes & Development, 30(1), 18–33. 10.1101/gad.267757.115 [PubMed: 26679841]

Fessé P, Nyman J, Hermansson I, Book M-L, Ahlgren J, & Turesson I. (2022). Human cutaneous interfollicular melanocytes differentiate temporarily under genotoxic stress. IScience, 25(10), 105238. 10.1016/j.isci.2022.105238

Gargiulo G, Cesaroni M, Serresi M, de Vries N, Hulsman D, Bruggeman SW, Lancini C, & van Lohuizen M. (2013). In Vivo RNAi Screen for BMI1 Targets Identifies TGF-β/BMP-ER Stress Pathways as Key Regulators of Neural- and Malignant Glioma-Stem Cell Homeostasis. Cancer Cell, 23(5), 660–676. 10.1016/j.ccr.2013.03.030 [PubMed: 23680149]

Ginjala V, Nacerddine K, Kulkarni A, Oza J, Hill SJ, Yao M, Citterio E, van Lohuizen M, & Ganesan S. (2011). BMI1 is recruited to DNA breaks and contributes to DNA damage-induced H2A ubiquitination and repair. Molecular and Cellular Biology, 31(10), 1972–1982. 10.1128/MCB.00981-10 [PubMed: 21383063]

Harris ML, Buac K, Shakhova O, Hakami RM, Wegner M, Sommer L, & Pavan WJ. (2013). A Dual Role for SOX10 in the Maintenance of the Postnatal Melanocyte Lineage and the Differentiation of Melanocyte Stem Cell Progenitors. PLoS Genetics, 9(7), e1003644. 10.1371/journal.pgen.1003644

Huang JM, & Hornyak TJ. (2015). Polycomb group proteins—Epigenetic repressors with emerging roles in melanocytes and melanoma. Pigment Cell & Melanoma Research, 28(3), 330–339. 10.1111/pcmr.12341 [PubMed: 25475071]

Inomata K, Aoto T, Binh NT, Okamoto N, Tanimura S, Wakayama T, Iseki S, Hara E, Masunaga T, Shimizu H, & Nishimura EK. (2009). Genotoxic stress abrogates renewal of melanocyte stem cells by triggering their differentiation. Cell, 137(6), 1088–1099. 10.1016/j.cell.2009.03.037 [PubMed: 19524511]

Iwama A, Oguro H, Negishi M, Kato Y, Morita Y, Tsukui H, Ema H, Kamijo T, Katoh-Fukui Y, Koseki H, van Lohuizen M, & Nakauchi H. (2004). Enhanced Self-Renewal of Hematopoietic Stem Cells Mediated by the Polycomb Gene Product Bmi-1. Immunity, 21(6), 843–851. 10.1016/j.immuni.2004.11.004 [PubMed: 15589172]

Jacobs JJL, Kieboom K, Marino S, DePinho RA, & van Lohuizen M. (1999a). The oncogene and Polycomb-group gene bmi-1 regulates cell proliferation and senescence through the ink4a locus. Nature, 397(6715), 164–168. 10.1038/16476 [PubMed: 9923679]

Jacobs JJ, Scheijen B, Voncken JW, Kieboom K, Berns A, & van Lohuizen M. (1999b). Bmi-1 collaborates with c-Myc in tumorigenesis by inhibiting c-Myc-induced apoptosis via INK4a/ARF. Genes & Development, 13(20), 2678–2690. [PubMed: 10541554]

Lessard J, & Sauvageau G. (2003). Bmi-1 determines the proliferative capacity of normal and leukaemic stem cells. Nature, 423(6937), 255–260. 10.1038/nature01572 [PubMed: 12714970]

Li H, & Hou L. (2018). Regulation of melanocyte stem cell behavior by the niche microenvironment. Pigment Cell & Melanoma Research, 31(5), 556–569. 10.1111/pcmr.12701 [PubMed: 29582573]

Liu J, Cao L, Chen J, Song S, Lee IH, Quijano C, Liu H, Keyvanfar K, Chen H, Cao L-Y, Ahn B-H, Kumar NG, Rovira II, Xu X-L, van Lohuizen M, Motoyama N, Deng C-X, & Finkel T. (2009). Bmi1 regulates mitochondrial function and the DNA damage response pathway. Nature, 459(7245), 387–392. 10.1038/nature08040 [PubMed: 19404261]

Mariani SA, Minieri V, De Dominici M, Iacobucci I, Peterson LF, & Calabretta B. (2016). CDKN2A-independent role of BMI1 in promoting growth and survival of Ph+ acute lymphoblastic leukemia. Leukemia, 30(8), 1682–1690. 10.1038/leu.2016.70 [PubMed: 27125204]

Maynard MA, Ferretti R, Hilgendorf KI, Perret C, Whyte P, & Lees JA. (2014). Bmi1 is required for tumorigenesis in a mouse model of intestinal cancer. Oncogene, 33(28), 3742–3747. 10.1038/onc.2013.333 [PubMed: 23955081]

Molofsky AV, He S, Bydon M, Morrison SJ, & Pardal R. (2005). Bmi-1 promotes neural stem cell self-renewal and neural development but not mouse growth and survival by repressing the p16Ink4a and p19Arf senescence pathways. Genes & Development, 19(12), 1432–1437. 10.1101/gad.1299505 [PubMed: 15964994]

Mort RL, Jackson IJ, & Patton EE. (2015). The melanocyte lineage in development and disease. Development, 142(4), 620–632. 10.1242/dev.106567 [PubMed: 25670789]

Nishimura EK. (2011). Melanocyte stem cells: A melanocyte reservoir in hair follicles for hair and skin pigmentation. Pigment Cell & Melanoma Research, 24(3), 401–410. 10.1111/j.1755-148X.2011.00855.x [PubMed: 21466661]

Nishimura EK, Granter SR, & Fisher DE. (2005). Mechanisms of hair graying: Incomplete melanocyte stem cell maintenance in the niche. Science (New York, N.Y.), 307(5710), 720–724. 10.1126/science.1099593 [PubMed: 15618488]

Oguro H, Iwama A, Morita Y, Kamijo T, van Lohuizen M, & Nakauchi H. (2006). Differential impact of Ink4a and Arf on hematopoietic stem cells and their bone marrow microenvironment in Bmi1-deficient mice. Journal of Experimental Medicine, 203(10), 2247–2253. 10.1084/jem.20052477 [PubMed: 16954369]

Park I, Qian D, Kiel M, Becker MW, Pihalja M, Weissman IL, Morrison SJ, & Clarke MF. (2003). Bmi-1 is required for maintenance of adult self-renewing haematopoietic stem cells. Nature, 423(6937), 302–305. 10.1038/nature01587 [PubMed: 12714971]

Pietersen AM, Evers B, Prasad AA, Tanger E, Cornelissen-Steijger P, Jonkers J, & van Lohuizen M. (2008). Bmi1 Regulates Stem Cells and Proliferation and Differentiation of Committed Cells in Mammary Epithelium. Current Biology, 18(14), 1094–1099. 10.1016/j.cub.2008.06.070 [PubMed: 18635350]

Pshenichnaya I, Schouwey K, Armaro M, Larue L, Knoepfler PS, Eisenman RN, Trumpp A, Delmas V, & Beermann F. (2012). Constitutive gray hair in mice induced by melanocyte-specific deletion of c-Myc. Pigment Cell & Melanoma Research, 25(3), 312–325. 10.1111/j.1755-148X.2012.00998.x [PubMed: 22420299]

Rabbani P, Takeo M, Chou W, Myung P, Bosenberg M, Chin L, Taketo MM, & Ito M. (2011). Coordinated Activation of Wnt in Epithelial and Melanocyte Stem Cells Initiates Pigmented Hair Regeneration. Cell, 145(6), 941–955. 10.1016/j.cell.2011.05.004 [PubMed: 21663796]

Steingrímsson E, Copeland NG, & Jenkins NA. (2005). Melanocyte stem cell maintenance and hair graying. Cell, 121(1), 9–12. 10.1016/j.cell.2005.03.021 [PubMed: 15820674]

Tonks ID, Nurcombe V, Paterson C, Zournazi A, Prather C, Mould AW, & Kay GF. (2003). Tyrosinase-Cre mice for tissue-specific gene ablation in neural crest and neuroepithelial-derived tissues. Genesis (New York, N.Y.: 2000), 37(3), 131–138. 10.1002/gene.10242 [PubMed: 14595836]

van der Lugt NM, Domen J, Linders K, van Roon M, Robanus-Maandag E, te Riele H, van der Valk M, Deschamps J, Sofroniew M, & van Lohuizen M. (1994). Posterior transformation, neurological abnormalities, and severe hematopoietic defects in mice with a targeted deletion of the bmi-1 proto-oncogene. Genes & Development, 8(7), 757–769. 10.1101/gad.8.7.757 [PubMed: 7926765]

van Lohuizen M, Verbeek S, Scheijen B, Wientjens E, van der Gulden H, & Berns A. (1991). Identification of cooperating oncogenes in E mu-myc transgenic mice by provirus tagging. Cell, 65(5), 737–752. [PubMed: 1904008]

Zaidi MR, Hornyak TJ, & Merlino G. (2011). A genetically engineered mouse model with inducible GFP expression in melanocytes. Pigment Cell & Melanoma Research, 24(2), 393–394. 10.1111/j.1755-148X.2011.00832.x [PubMed: 21392368]

Significance

Genetically engineered mouse models characterized by hair greying enable identification of genes important for melanocyte biology. Here, we identify BMI1, a regulator of self-renewal programs in numerous adult stem cell populations, as playing a key role in the maintenance of melanocyte stem cells (McSCs). Specifically, deletion of BMI1 in the melanocyte lineage results in progressive depletion of McSCs, thereby causing melanocyte loss and premature hair greying. We postulate that BMI1 enables McSC survival in part through silencing of the *Cdkn2a* locus, as well as through a non-canonical role in mitigating oxidative stress.

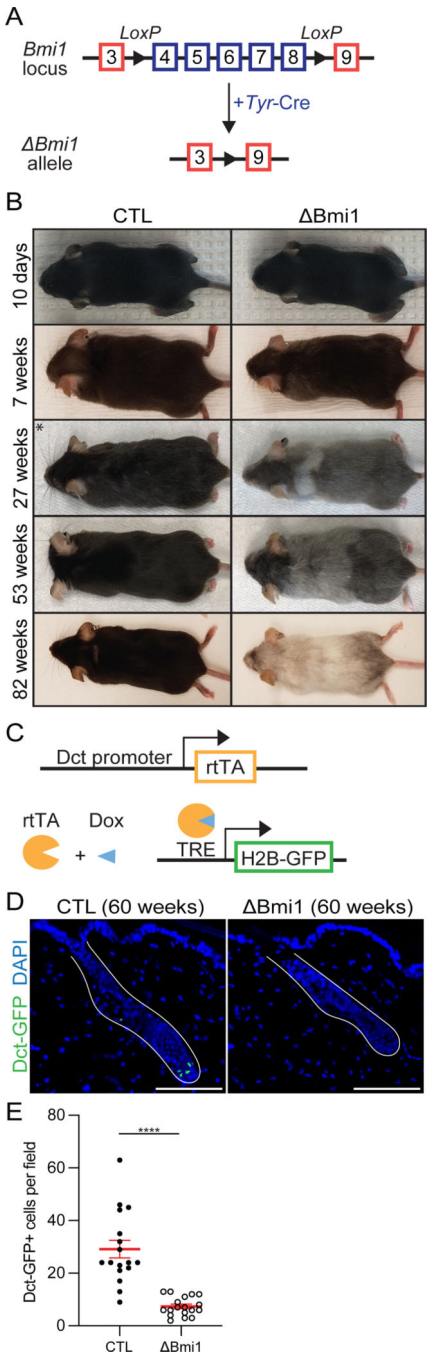

Figure 1. Phenotypic characterization of melanocyte-specific *Bmi1* deletion in mice.

(A) Schematic of floxed exons 4 through 8 of the conditional *Bmi1* allele undergoing *Tyr*-Cre-mediated recombination to yield *Bmi1* deletion (ΔBmi1). **(B)** Representative photos of ΔBmi1 (right) and littermate control (left) mouse coat color at indicated ages. The controls were all $Bmi1^{fl/fl}$ without *Tyr*-Cre (CTL) except for the 27-week-old littermate control (*), which was genotype $Bmi1^{fl/+}$; *Tyr*-Cre^{+}. Progressive loss of hair pigmentation is evident in the ΔBmi1 animals. **(C)** Schematic of bi-transgenic, doxycycline-inducible Dct-rtTA/TRE-H2B-GFP system that enables nuclear GFP expression in melanocyte-lineage cells

(Dct-GFP). **(D)** Fluorescence microscopy images (10X) of representative CTL (left) and ΔBmi1 (right) 60-week-old mouse skin sections labeled with DAPI and Dct-GFP, marking all nuclei (blue) and melanocyte-lineage cells (green), respectively. Hair follicles outlined in white. Scale bars, 100 μm. **(E)**. Dct-GFP^{+} melanocyte lineage cells were quantified by analysis of 5000×1300 pixel fields from 17 different skin sections from 2 CTL mice, and 18 different skin sections from 2 ΔBmi1 mice.

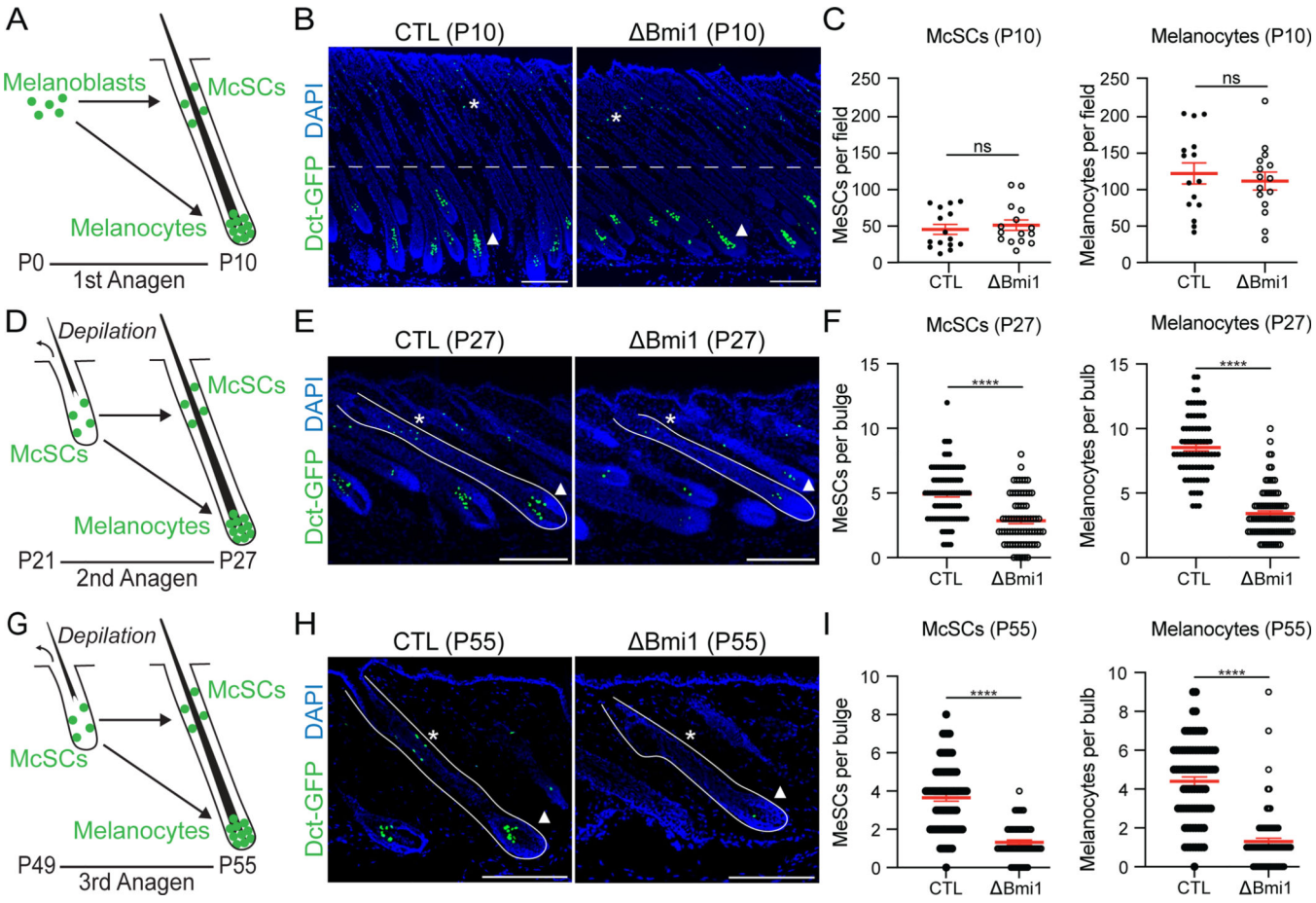

Figure 2. *Bmi1* deletion causes loss of McSCs and melanocytes during hair cycle progression.

(A-C) Dct-GFP$^+$ McSCs and melanocytes from CTL and ΔBmi1 mice were quantified during anagen of the first hair cycle. **(A)** Schematic of melanocyte lineage cell fate specification in the first anagen. **(B)** Representative fluorescence microscopy images (10X) of CTL (left) and ΔBmi1 (right) P10 mouse skin sections labeled with DAPI and Dct-GFP. Dashed line indicates separation of the hair follicle, with the upper region containing McSCs (*), and the lower region containing melanocytes (▲). Scale bars, 200 μm. **(C)** Upper Dct-GFP$^+$ McSCs and lower Dct-GFP$^+$ melanocytes were quantified by analysis of 5000×2000 pixel fields from 3 different skin sections per mouse, and 5 mice per genotype. The representation of CTL and ΔBmi1 melanocyte lineage cells was not significantly different. **(D-I)** Dct-GFP$^+$ McSCs and melanocytes from CTL and ΔBmi1 mice were quantified for the **(D-F)** second hair cycle, and **(G-I)** third hair cycle. **(D, G)** Schematics of the experimental scheme, showing depilation of hair shaft at the indicated timepoints to trigger telogen hair follicles to enter 2nd or 3rd anagen and cause McSCs to synchronously divide and both self-renew and give rise to mature melanocytes at the indicated terminal timepoints. **(E, H)** Representative fluorescence microscopy images (10X) of CTL (left) and ΔBmi1 (right) mouse skin sections labeled with DAPI and Dct-GFP at **(E)** 2nd anagen (P27) and **(H)** 3rd anagen (P55). Representative single hair follicles are outlined in white, with the position of McSCs (*) and melanocytes (▲) indicated. Scale bars, 200 μm. **(F, I)** Melanocyte lineage cells were quantified by identifying full cross-sections of hair follicle bulges and bulbs to

identify McSCs and melanocytes, respectively. In both the 2nd and 3rd anagen, the numbers of McSCs and melanocytes were significantly lower in the ΔBmi1 samples versus their CTL counterparts. **(F)** For the 2nd anagen (P27), we analyzed: 4 CTL mice, with a sum of 89 hair follicles for McSC representation and 81 hair follicles for melanocyte representation; and 3 ΔBmi1 mice, with a sum of 72 hair follicles for McSC representation and 89 hair follicles for melanocyte representation. **(I)** For the 3rd anagen (P55), we analyzed: 8 CTL mice, with a sum of 94 hair follicles for McSC representation and 83 hair follicles for melanocyte representation; and 5 ΔBmi1 mice, with a sum of 60 hair follicles for McSC representation and 75 hair follicles for melanocyte representation. For all graphs, the red bars indicate means ± SEM. “ns” indicates not statistically significant, and **** denotes $p \leq 0.0001$.

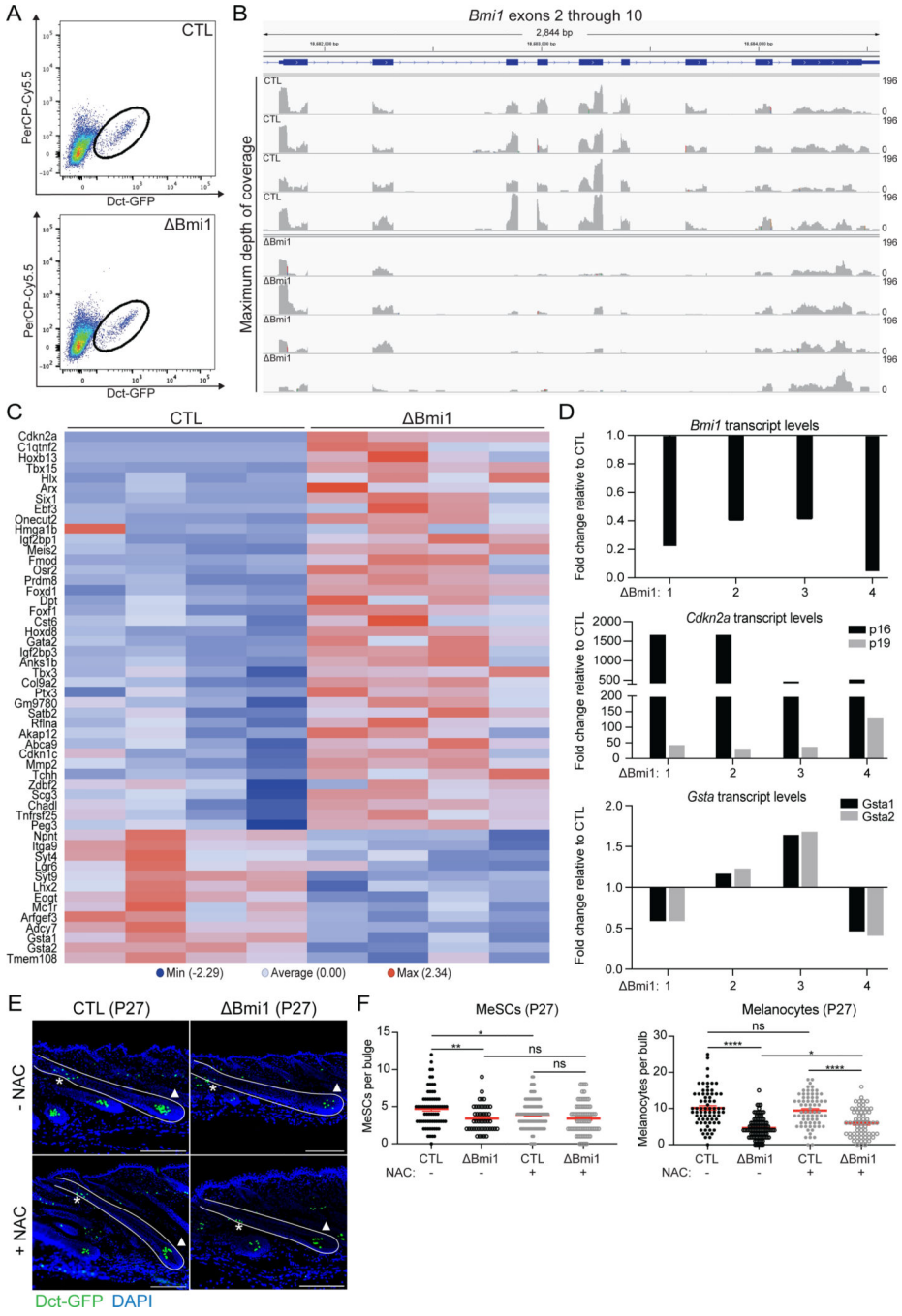

Figure 3. BMI1 regulates expression of Cdkn2a locus and ROS homeostasis genes in McSCs.

(A) Dct-GFP^{+}, PerCP-Cy5.5^{-} (non-autofluorescent) cells were isolated by FACS from freshly dissociated P21 mouse skin. **(B, C)** Gene expression was analyzed by RNA-seq for 4 CTL and 4 ΔBmi1 McSC samples. **(B)** STAR alignment of *Bmi1* reads to the murine *Bmi1* locus. **(C)** Heatmap showing differentially expressed genes ($\log_2$ fold change > 1, adjusted *p* value < 0.05). Color bar indicates Z-score. **(D)** New McSC samples were generated from 4 CTL and 4 ΔBmi1 mice, and analyzed by qRT-PCR to determine the levels of *Bmi1*, *Cdkn2a*, and *Gsta1/2* transcripts, normalized to *Gapdh* as an internal control. The graphs

show the normalized levels for each ΔBmi1 sample, relative to the average of the normalized levels for the 4 CTL samples. **(E)** Fluorescence microscopy images (10X) of CTL (left) and ΔBmi1 (right) P27 skin sections from mice administered either normal (-NAC) water or 1 mg/mL NAC (+NAC) water from P0-P27. Sections are labeled with DAPI and Dct-GFP. A single hair follicle, outlined in white, contains McSCs (*) and melanocytes (▲). Scale bars, 200 μm. **(F)** Melanocyte lineage cells were quantified as described in Figure 2 (F, I) using: 5 CTL –NAC mice (71 hair follicles for McSCs and 71 hair follicles for melanocytes); 5 ΔBmi1 –NAC mice (47 hair follicles for McSCs and 105 hair follicles for melanocytes); 5 CTL +NAC mice (104 hair follicles for McSCs and 70 hair follicles for melanocytes) and 5 ΔBmi1 +NAC mice (78 hair follicles for McSCs and 64 hair follicles for melanocytes). The red bars indicate means ± SEM, where $p \leq 0.05$ (*), $p \leq 0.01$ (**), $p \leq 0.001$ (***), and $p \leq 0.0001$ (****) were considered statistically significant, and “ns” indicates not statistically significant.